PHYSICAL REVIEW B VOLUME 21, NUMBER 10 15 MAY 1980

Self-consistent cluster theory for systems with off-diagonal disorder

Theodore Kaplan
Solid State Division, Oak Rdige National Laboratory, Oak Ridge, Tennessee 37830

P. L. Leath
Serin Physics Laboratory, Rutgers University, Piscataway, New Jersey 08854

L. J. Gray
Mathematics and Statistics Research Department, Union Carbide Corporation Nuclear Division, Oak Ridge, Tennessee 37830

H. W. Diehl*
Serin Physics Laboratory, Rutgers University, Piscataway, New Jersey 08854

(Received 23 October 1979)

A self-consistent cluster theory for elementary excitations in systems with diagonal, off-diagonal, and environmental disorder is presented. The theory is developed in augmented space where the configurational average over the disorder is replaced by a ground-state matrix element in a translationally invariant system. The analyticity of the resulting approximate Green's function is proved. Numerical results for the self-consistent single-site and pair approximations are presented for the vibrational and electronic properties of disordered linear chains with diagonal, off-diagonal, and environmental disorder.

I. INTRODUCTION

A substitutional defect at site i in a crystal generally produces three types of changes in the system Hamiltonian. These are diagonal changes V_{ii}, off-diagonal changes V_{ij} (where j is some neighboring site), and environmental changes V_{jk} in the vicinity of the defect. In the electronic tight-binding model the diagonal perturbations correspond to changes in the energy level at the defect site, the off-diagonal part to changes in the interatomic hopping to and from the defect site, and the environmental part to energy level and hopping changes in the vicinity of the defect due to such effects as charge transfer and lattice relaxation. In the case of phonons and spin waves, all three types of perturbations or disorder are coupled by the general translational or rotational symmetry of the system.

In recent years there have been many attempts to develop adequate approximations for the properties of disordered systems.[1] The first successful, self-consistent approximation was the coherent potential approximation (CPA) developed for the electronic problem by Soven[2] and for the phonon case by Taylor[3] in 1967. The CPA is a self-consistent, single-site approximation for alloys with diagonal disorder. In the tight-binding electronic model with diagonal and off-diagonal disorder (but without environmental disorder) a successful single-site generalization was produced by Blackman *et al.*[4] These approximations are translationally invariant and give analytic (or, more properly, Herglotz) Green's functions for all degrees of the disorder. Over the next several years, there were many attempts to generalize these self-consistent methods so as to include off-diagonal and environmental disorder (as required by disordered force constants in the phonon problem and disordered exchange in the spin-wave problem) and to allow multisite or cluster scattering. Only in certain very special cases, such as the separable[5] or the additive[6,7] limits of off-diagonal and environmental disorder, was there any success. The more general approximations[8-10] produced Green's functions which failed to retain the Herglotz nature, the translational invariance of the averaged system, or were not fully self-consistent, and were thus unsuitable for calculating spectral density functions or such transport properties as the location and existence of mobility edges.

Very recently, Mills and Ratanavararaksa,[11] using diagrammatic methods, have developed an extension of the CPA which, although restricted to the diagonal disorder problem, does provide a successful self-consistent multisite scattering theory. This approximation was rederived using the operator methods of the augmented-space formalism[12-14] (ASF) by Diehl and Leath[15] (for binary alloys), and generalized to multicomponent systems by Mills and Ratanavararaksa.[11] Furthermore, Mills's proof of analyticity is based upon this augmented-space representation. In developing their traveling cluster approximation, Mills and Ratanavararaksa[11] introduced a diagram symmetry rule which gives a sufficient condition for constructing a self-energy with a negative-definite imaginary part. Mills's symmetry rule and the augmented-space techniques of Mookerjee[12] and

Kaplan and Gray[13, 14] were then combined by Diehl and Leath[16] to describe a perturbation theory for phonons with disordered force constants. The particular self-consistent approximation illustrated by Diehl and Leath is analytic and translationally invariant, but neglects a significant part of the off-diagonal disorder, resulting in an approximation which is similar in structure to the additive limit CPA. In a further application of this theory by Diehl *et al.*,[17] an extension of the t-matrix approximation (ATA) (Refs. 18, 19) to the case of force constant disorder was constructed. All significant off-diagonal terms are included in this approximation but in a non-self-consistent form.

In the present work, we use a similar approach based on the augmented-space formalism[12-14] and the approximation of Mills and Ratanavararaksa[11] to develop a fully self-consistent cluster theory for elementary excitations (electrons, phonons, magnons, excitons, etc.) in general disordered systems. This approach is sufficiently powerful that it produces analytic translationally invariant approximations at all concentrations for diagonal, off-diagonal, and environmental disorder including such possible future applications as charge transfer and lattice relaxation. This theory, which is developed in terms of an operator formalism rather than a diagrammatic expansion, is a true generalization of the work of Mills and Ratanavararaksa[11] to the general disorder problem. However, it falls short of a complete theory in that short-range order is not yet included. The theory is illustrated here by a calculation of the self-consistent single-site and pair approximations for electronic and vibrational spectra in systems with diagonal, off-diagonal, and environmental disorder.

In Sec. II we introduce the formalism, employing the augmented-space representation for random systems. As an aid to understanding the self-consistent approximation, a diagrammatic representation of the terms in the perturbation expansion is included. In Sec. III, the systematic self-consistent cluster approximations are described (with the proof of the analyticity of these approximations presented in Appendix A). In Secs. IV and V numerical results are presented for the single-site and nearest-neighbor pair approximations for electrons and phonons in one-dimensional systems. Concluding remarks are presented in Sec. VI.

II. FORMALISM

In this section, we briefly sketch the construction of augmented space and define the notation to be used throughout the remainder of the paper. The reader is referred to Ref. 13 for a more detailed description.

All types of excitations in disordered systems may be discussed by the same theoretical methods.[1] In this section, we have chosen for simplicity to present our discussion in the notation of the electronic problem, occasionally indicating the appropriate equations for the phonon problem. To obtain the appropriate notation for other excitations, the reader is referred to Sec. II of Ref. 1.

We assume that the lattice sites are randomly occupied by atoms of type A, B, C, etc. The random variable s_l is defined to take on the value A, B, or C, etc., corresponding to the occupation of site l. (For systems with continuous disorder, s_l takes on a continuous range of values.) We assume that the $\{s_l\}$ are independent random variables with probability distribution $p(s_l)$. [The more general case of dependent variables[14] (short-range order) is not treated.]

We wish to calculate the configuration-averaged values of physical quantities and the related Green's functions. In particular, we shall calculate the configuration-averaged one-particle Green's function

$$\bar{G}_{nm}(E)=\int\int\cdots\int G_{nm}(\{s_l\},E)\prod_l p(s_l)ds_l\,, \tag{2.1}$$

where, for the electronic problem, the one-electron Green's function for a particular configuration is

$$G_{nm}(\{s_l\},E)=\langle\psi_n|[EI-H(\{s_l\})]^{-1}|\psi_m\rangle\,, \tag{2.2}$$

and for the phonon system, the displacement-displacement Green's function is

$$G_{nm}(\{s_l\},\omega)=\langle\psi_n|[\omega^2M(\{s_l\})-\Phi(\{s_l\})]^{-1}|\psi_m\rangle\,. \tag{2.3}$$

Here, $|\psi_n\rangle$ is a basis for the Hilbert space Ψ and the integration over $p(s_l)ds_l$ constitutes averaging over all possible configurations of the disordered system.

The Hamiltonian H in Eq. (2.2) and the mass M and force constant Φ matrices in Eq. (2.3) are explicit functions of the variables $\{s_l\}$, and can be decomposed into a nonrandom part H_0, and terms which depend on the occupation of 1, 2, . . . , etc. sites; i.e.,

$$H(\{s_l\})=H_0+\sum_i\sum_s V^i(s)\delta(s_i,s)+\sum_{i\neq j}\sum_{s,s'}V^{ij}(s,s')\delta(s_i,s)\delta(s_j,s')+\dots\,, \tag{2.4}$$

where s denotes the type of atom, $\sum_s$ is over all atom types, and $\delta(s_i,s)$ is the Kronecker delta function. In the augmented-space formalism, the random variables $\{s_l\}$ are replaced by operators $\{\hat{S}_l\}$ acting on a Hilbert space Θ (the "disorder" space). Functions of the random variables are replaced by functions of the corresponding operators, and thus the Kronecker functions $\delta(s_i,s)$ become spectral projection operators $\hat{\delta}(\hat{S}_l,s\hat{I})$. For a binary A-B alloy, $\hat{S}_l$ will have only two eigenvalues corresponding to the two possibilities of the occupation of site l. The space Θ can be conveniently written as a direct product, $\Theta = \prod_l \theta_l$, where there is a Hilbert space θ_l for each variable s_l. A basis for Θ is given by vectors of the form $\prod_l |s\rangle_l$, where $|s\rangle_l$ belongs to θ_l, and can be $|A\rangle_l, |B\rangle_l, \ldots$, etc. Thus, for a binary alloy, each θ_l is two dimensional. Note that each basis vector $\prod_l |s\rangle_l$ corresponds to a particular configuration of the solid. The spectral projection operators $\hat{\delta}(\hat{S}_l,s\hat{I})$ act on Θ and are given by

$$\begin{aligned}\hat{\delta}(\hat{S}_l,A\hat{I})\prod_i |s\rangle_i &= \delta(s_l,A)\prod_i |s\rangle_i\,,\\ \hat{\delta}(\hat{S}_l,B\hat{I})\prod_i |s\rangle_i &= \delta(s_l,B)\prod_i |s\rangle_i, \ldots\,,\end{aligned} \tag{2.5}$$

where $\delta(s_l,A)=1$ if $|s\rangle_l = |A\rangle_l$ and zero otherwise. The augmented space Ω is the product of Θ with the "real" space, Ψ, $\Omega = \Psi \otimes \Theta$, and the substitution of the projection operators defined in (2.5) for the Kronecker functions in Eq. (2.4) defines the augmented-space Hamiltonian $\hat{H}$ on the space Ω. Thus the augmented space is spanned by the vectors

$$|\psi_i\rangle \prod_l |s\rangle_l = |i; s_1, s_2, \ldots, s_l, \ldots\rangle\,,$$

where $\{|\psi_i\rangle\}$ span Ψ.

The augmented-space one-electron and one-phonon Green's functions are $\hat{G}(E) = (E\hat{I} - \hat{H})^{-1}$ and $\hat{G}(\omega) = (\hat{M}\omega^2 - \hat{\Phi})^{-1}$, respectively. In this notation, the Green's function for a particular configuration of site occupations $\{s_l\}$ in the solid corresponds to the matrix element

$$G_{nm}(\{s_l\}) = \langle n; s_1, s_2, \ldots |\hat{G}| m; s_1, s_2, \ldots\rangle\,. \tag{2.6}$$

In order to calculate configuration averages, we must choose the appropriate representation. In each θ_l we let

$$|0\rangle_l \equiv \sum_s [p(s)]^{1/2} |s\rangle_l\,, \tag{2.7}$$

so that each species occurs with its appropriate probability. In Ω we define the vector

$$|nf\rangle \equiv |\psi_n\rangle \prod_l |0\rangle_l = |\psi_n\rangle |f\rangle\,. \tag{2.8}$$

We designate $|0\rangle_l$ as the *unexcited state* in θ_l and $|f\rangle$ as the *ground state* of the disorder space Θ. The configuration average of the Green's function (or any other quantity) becomes the ground-state matrix element

$$\overline{G}_{nm}(E) = \langle nf|\hat{G}(E)|mf\rangle\,. \tag{2.9}$$

For a binary A-B alloy, with a concentration $c_A = p(A)$ of A atoms and $c_B = p(B) = 1 - c_A$ of B atoms, there are only two basis vectors for θ_l,

$$|0\rangle_l = \sqrt{c_A}\,|A\rangle_l + \sqrt{c_B}\,|B\rangle_l\,, \tag{2.10a}$$

$$|1\rangle_l = \sqrt{c_B}\,|A\rangle_l - \sqrt{c_A}\,|B\rangle_l\,; \tag{2.10b}$$

the vector $|1\rangle_l$ is orthogonal to $|0\rangle_l$ and is called the *excited state at site l* (for multicomponent systems, there will be more than one excited state). In the standard notation for augmented space,[12,13] $|lf_{m,n,\ldots,p}\rangle$ specifies the vector in Ω where the sites $m, n, \ldots, p$ are in the excited state $|1\rangle$, and all other sites are in the state $|0\rangle$ (sites in the state $|1\rangle$ have also been referred to as sites with pseudofermions[15,17,20,21]). To further simplify notation, the vector $|lf_{m,n,\ldots,p}\rangle$ will be written $|lf_\sigma\rangle$, where $\sigma = \{m, n, \ldots, p\}$ will specify which sites are in the excited state.

The self-energy Σ is defined by the usual relation

$$\overline{G}(E) = [G_{\text{vc}}^{-1}(E) - \Sigma(E)]^{-1}\,, \tag{2.11}$$

where $G_{\text{vc}}(E) = (E - \overline{H})^{-1}$ or $(\overline{M}\omega^2 - \overline{\Phi})^{-1}$, for the electron or phonon problem, respectively. Here, $\overline{H}$, $\overline{M}$, and $\overline{\Phi}$ denote the configuration-averaged operators. In order to simplify the notation in what follows, we will consider a binary A-B alloy. The extension to ternary and other multicomponent systems is straightforward.[12]

Any operator $\hat{A}$ in augmented space can be represented in the block form

$$\hat{A} = \begin{bmatrix} \overline{A} & A' \\ A'^{\dagger} & \tilde{A} \end{bmatrix}, \tag{2.12}$$

where $\overline{A} = P\hat{A}P$, $A' = P\hat{A}(1-P)$, $A'^{\dagger} = (1-P)\hat{A}P$, and $\tilde{A} = (1-P)\hat{A}(1-P)$, with P being the projection operator onto all the ground-state vectors

$$P = \sum_i |if\rangle\langle if|\,. \tag{2.13}$$

From (2.9) we see that $\overline{A}$ is the configuration average of the physical quantity $\hat{A}$. In this block form, we can easily take the matrix inverse of $\hat{K} = E\hat{I} - \hat{H}$ and calculate the upper left block $\overline{G}$ of $\hat{G}$. With the use of (2.11), we obtain

$$\Sigma = K'FK'^{\dagger}\,, \tag{2.14}$$

where

$$F=\tilde{K}^{-1}=[(G_{\text{vc}})^{-1}\tilde{I}-\tilde{V}]^{-1}, \tag{2.15}$$

and where

$$\tilde{V}=\overline{K}\tilde{I}-\tilde{K}. \tag{2.16a}$$

For the electron and phonon problems we have

$$\tilde{V}=\tilde{H}-\overline{H}\tilde{I} \tag{2.16b}$$

and

$$\tilde{V}=(\overline{M}\tilde{I}-\tilde{M})\omega^2-(\overline{\Phi}\tilde{I}-\tilde{\Phi}), \tag{2.16c}$$

respectively. (Note that by $\overline{K}\tilde{I}$ we mean $\langle if_\sigma|\overline{K}\tilde{I}|jf_{\sigma'}\rangle=\overline{K}_{ij}\delta^{\sigma\sigma'}$, where σ and σ' are not the null set.)

In the remainder of the paper we use the simplified notation

$$\langle if_\sigma|\hat{A}|jf_{\sigma'}\rangle=A_{ij}^{\sigma\sigma'}. \tag{2.17}$$

If the i and j indices are suppressed, then matrix operations over real-space indices are understood. If σ is the null set (i.e., the ground state), then it will be omitted. This occurs, for example, with the K' operator

$$\langle f|\hat{K}|f_\sigma\rangle=K'^{\sigma}, \tag{2.18a}$$

$$\langle f_\sigma|\hat{K}|f\rangle=K'^{\dagger\sigma}. \tag{2.18b}$$

In this notation the equations for the self-energy [Eqs. (2.14) and (2.15)] are

$$\Sigma=\sum_{\sigma,\sigma'}K'^{\sigma}F^{\sigma\sigma'}K'^{\dagger\sigma'}, \tag{2.19}$$

and

$$F^{\sigma\sigma'}=G_{\text{vc}}\left(\delta^{\sigma\sigma'}+\sum_{\sigma''}\tilde{V}^{\sigma\sigma''}F^{\sigma''\sigma'}\right). \tag{2.20}$$

In the following section, we use operator techniques to generate a self-consistent approximation for the configuration-averaged one-particle Green's function. As an aid to the reader in visualizing the scattering terms included, we also introduce a diagram description of the problem by iterating Eqs. (2.19) and (2.20) to produce the perturbation expansion of $\hat{G}$ about the virtual crystal G_{vc} in powers of $\tilde{V}$ and K'. The terms in this expansion can be represented by diagrams such as those in Fig. 1. (The particular diagrams presented are for a linear chain with nearest-neighbor hopping.) In these graphs the solid circles represent the sites of the excitations (or psuedofermions). The first vertical vertex line on the left represents K' and the open circles correspond to the two sites neighboring the excitation site where K' has nonzero matrix elements. Similarly, the last vertical vertex line on the right of each diagram represents $K'^{\dagger}$, and the intermediate vertices represent the perturbation matrices $\tilde{V}$. The horizontal lines are excitation lines with which one associates a matrix propagator G_{vc}. Since we are considering a Hamiltonian which includes the terms shown in Eq. (2.4), $\hat{H}$ is quadratic in $\hat{\delta}$, and either one or two excitation lines may be created (or annihilated) by K' (or $K'^{\dagger}$), and the matrix $\tilde{V}$ which gives the scattering by the excitations may either leave them at the same sites or move them to neighboring sites or even create or destroy one of the excitations as long as one or two excitations enter and leave each $\tilde{V}$ vertex line. A self-consistent approximation is constructed by operator techniques and diagrammatically illustrated in Sec. III. Mills's diagram symmetry rule, which ensures that $\text{Im}\Sigma<0$, is reviewed briefly in Appendix B.

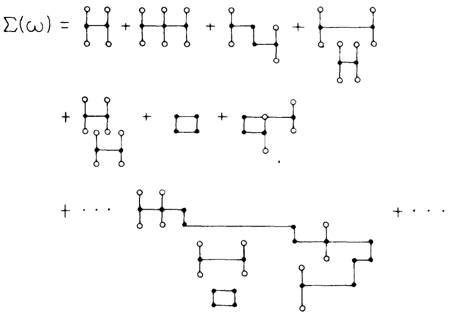

FIG. 1. Diagrammatic expansion of the self-energy for a linear chain with nearest-neighbor interactions. The solid circles represent sites with excitations (pseudofermions) and the open circles above and below represent the nearest neighbors where K' and $\tilde{V}$ have nonzero matrix elements.

III. SELF-CONSISTENT CLUSTER APPROXIMATIONS

In this section we develop an approximate method for evaluating the self-energy, taking into account the scattering by clusters of excitations. We proceed by dividing augmented space into two subspaces; one subspace S_T is treated exactly, while the orthogonal complement is only approximated. The subspace S_T is spanned by the vectors $|if_\sigma\rangle$, where i ranges over all sites, $\sigma\in T$, and T is the collection or family of excitation states which define the particular approximation. For example, in the single-site approximation, T is the set of states which have an excitation (or pseudofermion) on just one site. In the nearest-neighbor pair approximation, T is the set of states with no more than two nearest-neighbor sites having excitations, and in more general cluster approximations, T defines those clusters on which excitations are allowed (or those clusters of sites whose scattering is to be calculated).

The particular cluster approximation desired is derived by treating the scattering by the excitations within S_T exactly. In particular, we restrict the intermediate excitation states in Eqs. (2.19) and (2.20) to those in S_T. We thus obtain

$$\Sigma = \sum_{\sigma, \sigma' \in T} K'^{\sigma} F^{\sigma\sigma'} K'^{\dagger\sigma'}, \tag{3.1}$$

and

$$F^{\sigma\sigma'} = G_{\mathrm{vc}} \left(\delta^{\sigma\sigma'} + \sum_{\sigma'' \in T} \tilde{V}^{\sigma\sigma''} F^{\sigma''\sigma'} \right). \tag{3.2}$$

These equations define the *non-self-consistent* cluster approximations for the self-energy. For example, if T is the set of all single sites, i.e., $T = \{\sigma | \sigma = \{i\}\}$, and only diagonal disorder is present, we obtain the ATA (Refs. 18,19) (non-self-consistent single-site approximation). If we choose the more general Hamiltonian with off-diagonal and environmental disorder, we obtain the generalization of the ATA previously called the traveling pseudofermion approximation.[17] Similarly, the ATA is easily extended to pairs or clusters by enlarging S_T. From Eq. (3.1) we see that the self-energy Σ is a sum of terms of the form $XYX^\dagger$, where $\mathrm{Im}Y < 0$, as can be seen from Eq. (3.2). Thus, $\mathrm{Im}\Sigma < 0$. The averaged Green's function $\bar{G}$ is therefore Herglotz.

A major difference between this and previous approximations is that for extended scattering (by clusters or single excitations with off-diagonal and/or environmental disorder) the matrix $\tilde{V}$ has matrix elements which directly or indirectly shift the excitations from site to site giving rise to "traveling pseudofermions"[17] or, more generally, traveling cluster approximations. This feature allows the self-energy to have nonzero off-diagonal elements extending across the sample and thus contributes importantly to such quantities as the two-particle vertex corrections, in a way the CPA can not.

In order to produce an analytic *self-consistent approximation*, we replace G_{vc} in Eq. (3.2) by a self-consistent propagator G^σ which approximates the contribution from augmented space outside S_T. We rewrite Eq. (3.2) as, for $\sigma, \sigma' \in T$,

$$F^{\sigma\sigma'} = G^{\sigma} \left(\delta^{\sigma\sigma'} + \sum_{\sigma'' \in T} \tilde{V}^{\sigma\sigma''} F^{\sigma''\sigma'} \right), \tag{3.3}$$

where

$$G^\sigma = [(G_{\mathrm{vc}})^{-1} - \Sigma^\sigma]^{-1}. \tag{3.4}$$

Here, Σ^σ is the conditional self-energy which contains all those self-energy contributions to G^σ which are not included explicitly in Eq. (3.3), and which can be approximated in terms of the contributions from S_T, that is,

$$\Sigma^\sigma = \sum_{\alpha U\sigma \notin T,\, \alpha' U\sigma \notin T} K'^{\alpha} F^{\alpha\alpha'} K'^{\dagger\alpha'}, \tag{3.5}$$

with $\alpha, \alpha' \in T$. The restriction that both $\alpha U\sigma$ and $\alpha' U\sigma$ are not contained in T ensures that α and α' do not duplicate the scattering from sites σ accounted for explicitly in Eq. (3.3). The self-consistent set of equations (2.11), (3.1), (3.3), (3.4), and (3.5) define our self-consistent cluster theory for an approximate, configuration-averaged Green's function. It is shown in Appendix A that these equations have a unique solution which yields a Herglotz Green's function. A key to the analyticity is the symmetry of Eq. (3.5) with respect to α and α' (see Eq. A6). If the Hamiltonian contains only diagonal disorder these equations reduce to those of Mills and Ratanavararaksa.[11]

At this point, we indicate the necessity of using the augmented-space approach in solving this disorder problem. For the special case of diagonal disorder the simple form of the Hamiltonian allowed Mills and Ratanavararaksa[11] to express the self-consistency requirements in terms of restricted sums in real space [Eq. (5.2) of Ref. 11]. For the more general disorder problem treated here, this approach does not work. Instead, it is essential to impose self-consistency by means of restrictions in the full augmented space, as has been done in Eq. (3.5).

Since we are calculating the configuration-averaged Green's function, it is essential that the set $\{\sigma\}$ of sites and clusters contained in T be translationally invariant. This translational invariance is incorporated by writing T, for the η-cluster approximation, in the form

$$T = \{\sigma \,|\, \sigma = \sigma_1(i), \sigma_2(i), \ldots, \sigma_\eta(i), \forall i\}, \tag{3.6}$$

where $\sigma_m(i)$ is a particular cluster of sites at which there are excitations, defined relative to site i. Any other translationally equivalent cluster of sites can be generated by changing the index i. For example, in the nearest-neighbor pair approximation for a linear chain we choose $\sigma_1(i) = \{i\}$ and $\sigma_2(i) = \{i, i+1\}$.

In order to understand the approximations made in Eqs. (3.3)–(3.5) it is useful to consider the diagrammatic representation for simple examples. The single-site approximation is obtained by setting $T = \{\sigma \,|\, \sigma = \sigma_1(i) = \{i\}\}$ and is represented in Fig. 2. The upper line of diagrams represents the contributions from Eq. (3.3) which do not have self-energy insertions. These are equivalent to the single-site non-self-consistent approximation of Eq. (3.2). The lower line includes the self-energy insertions which are generated by the self-consistent propagator G^σ of Eq. (3.4). In order to prevent multiple occupancy (overcounting), the excitations in the self-energy insertion are con-

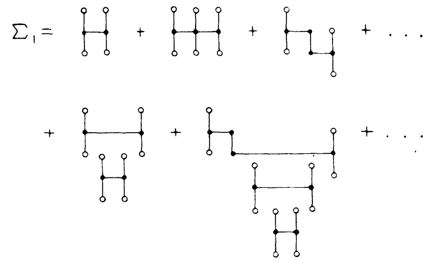

FIG. 2. Diagrammatic expansion of the self-energy in the self-consistent, single-site approximation where those diagrams which contain just one excitation are included (upper line) plus those that are included by the self-consistency (lower line).

strained not to be at the same sites as those of the line into which they are inserted. When the inserted excitation happens to be on the nearest-neighbor site of an existing excitation, there is a change in the matrix elements of the relevant K' and $\tilde{V}$ due to the previous excitation; this change is not included.

The nearest-neighbor pair approximation is illustrated diagrammatically in Fig. 3. A new feature in these diagrams is the simultaneous creation (or destruction) of two excitations on nearest-neighbor sites, which occurs because of the off-diagonal disorder.

It now remains to solve the self-consistent set of equations, making use of the translational symmetry of the augmented-space operators. We accomplish this by Fourier transforms on the disorder-space cluster-site labels. It is simplest to describe these transforms when we have chosen a specific basis set $\{|\psi_l\rangle\}$ for the original real-space Hamiltonian H. Since the tight-binding Hamiltonian is studied extensively in the theory of disordered systems, and since the model calculations presented in Secs. IV and V are for tight-binding systems, we consider a localized basis $|\psi_l\rangle$ where l refers to the lattice-site index. The matrix elements of the augmented-space operator $\hat{A}$ are of the general form $A_{m,n}^{\sigma_i(l),\sigma_j(l')}$, where $\sigma_i(l)$ represents a cluster of excitations as defined in Eq. (3.6).

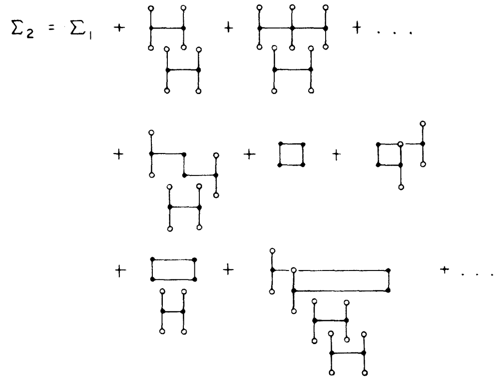

FIG. 3. Diagrammatic expansion of the self-energy in the self-consistent pair approximation where those diagrams which contain no more than two excitations at a time are included plus those that are included by the self-consistency.

The Fourier transform on the clusters σ is defined by

$$A(\vec{q})_{m,n}^{\sigma_i,\sigma_j} \equiv N^{-1} \sum_{l,l'} A_{l+m,\,l'+n}^{\sigma_i(l),\sigma_j(l')} e^{-i\vec{q}\cdot\vec{R}_{ll'}} \tag{3.7}$$

with the inverse relation

$$A_{l+m,\,l'+n}^{\sigma_i(l),\sigma_j(l')} = N^{-1} \sum_{\vec{q}} A(\vec{q})_{m,n}^{\sigma_i,\sigma_j} e^{i\vec{q}\cdot\vec{R}_{ll'}}, \tag{3.8}$$

where $\sigma_i \equiv \sigma_i(0)$, $\vec{R}_{ll'}$ is the lattice vector connecting the reference sites l and l' of the two clusters, and the $\vec{q}$ sum is over the Brillouin zone.

Of course, there is the usual Fourier transform on the real-space coordinates

$$\Sigma(\vec{q}) \equiv N^{-1} \sum_{ij} \Sigma_{ij} e^{-i\vec{q}\cdot\vec{R}_{ij}}. \tag{3.9}$$

Thus, Σ of Eq. (2.19) becomes

$$\Sigma(\vec{q}) = \sum_{ij} \sum_{l,m,n,p} K_{lm}'^{\sigma_i} F(\vec{q})_{mn}^{\sigma_i\sigma_j} K_{np}'^{\dagger\sigma_j} e^{-i\vec{q}\cdot\vec{R}_{lp}}. \tag{3.10}$$

In this notation, the transform $F(\vec{q})$ of Eq. (3.2) becomes

$$F(\vec{q})_{mn}^{\sigma_i\sigma_j} = G_{mn}^{\sigma_i}\delta^{\sigma_i\sigma_j} + \sum_{k,l,p} G_{ml}^{\sigma_i} \tilde{V}(\vec{q})_{lp}^{\sigma_i\sigma_k} F(\vec{q})_{pn}^{\sigma_k\sigma_j}. \tag{3.11}$$

Since the range of interaction in real space is finite, the perturbations K'^{σ_i} and $\tilde{V}(\vec{q})^{\sigma_i\sigma_j}$ are nonzero only over a finite set of real sites. We designate by P^{σ_i} the projection onto the union of these real sites.

For example, if there are interactions only between each site and each of its Z nearest neighbors, and if we are considering the single-site approximation, the $\tilde{V}(\vec{q})$ and K' are $(Z+1)\times(Z+1)$ matrices. This is the minimum dimension necessary to exhibit all the localized modes or states about each defect.

We next rewrite Eq. (3.11) in terms of projection operators P^{σ_i},

$$P^{\sigma_i}F(\vec{q})^{\sigma_i\sigma_j}P^{\sigma_j} = P^{\sigma_i}G^{\sigma_i}P^{\sigma_i}\delta_{ij} + \sum_{l} P^{\sigma_i}G^{\sigma_i}P^{\sigma_i}\tilde{V}^{\sigma_i\sigma_l}P^{\sigma_l}F^{\sigma_l\sigma_j}P^{\sigma_j}. \tag{3.12}$$

In order to evaluate G^{σ} we rewrite Eq. (3.4) as

$$G^{\sigma} = [(G_{vc})^{-1} - \Sigma^{\sigma}]^{-1} = (\bar{G}^{-1} + \tilde{\Sigma}^{\sigma})^{-1}, \tag{3.13}$$

where $\tilde{\Sigma}^{\sigma} = (\Sigma - \Sigma^{\sigma})$. Solving for $\tilde{\Sigma}^{\sigma}$ using Eqs.

(3.1) and (3.5), we obtain

$$\tilde{\Sigma}^{\sigma}=\sum_{\alpha U\sigma\in T,\text{ or }\alpha' U\sigma\in T} K'^{\alpha}F^{\alpha\alpha'}K'^{\dagger\alpha'} \tag{3.14a}$$

for α, $\alpha'\in T$, or

$$\tilde{\Sigma}^{\sigma}=\sum_{\alpha U\sigma\in T}\sum_{\alpha'}(K'^{\alpha}F^{\alpha\alpha'}K'^{\dagger\alpha'}+K'^{\alpha'}F^{\alpha'\alpha}K'^{\dagger\alpha})$$
$$-\sum_{\alpha U\sigma\in T,\ \alpha' U\sigma\in T} K'^{\alpha}F^{\alpha\alpha'}K'^{\dagger\alpha'} \tag{3.14b}$$

for α, $\alpha'\in T$. Then we break $\tilde{\Sigma}^{\sigma}$ into blocks: $\Sigma_1^{\sigma}\equiv P^{\sigma}\tilde{\Sigma}^{\sigma}P^{\sigma}$, $\Sigma_2\equiv(1-P^{\sigma})\tilde{\Sigma}^{\sigma}(1-P^{\sigma})$, and $\Sigma_3^{\sigma}\equiv P^{\sigma}\tilde{\Sigma}^{\sigma}\times(1-P^{\sigma})$. Similarly, we define $G_1\equiv P^{\sigma}\overline{G}P^{\sigma}$, $G_2\equiv(1-P^{\sigma})\overline{G}(1-P^{\sigma})$, and $G_3\equiv P^{\sigma}\overline{G}(1-P^{\sigma})$. Using Eq. (3.14), we find for α, $\alpha'\in T$

$$\Sigma_3^{\sigma}=\sum_{\alpha U\sigma\in T}\sum_{\alpha'}K'^{\alpha}F^{\alpha\alpha'}K'^{\dagger\alpha'}$$
$$-P^{\sigma}\Bigl(\sum_{\alpha U\sigma\in T}\sum_{\alpha'}K'^{\alpha}F^{\alpha\alpha'}K^{\dagger\alpha'}\Bigr)P^{\sigma}, \tag{3.15a}$$

and

$$\Sigma_2^{\sigma}=0\,. \tag{3.15b}$$

We can now solve for $P^{\sigma}G^{\sigma}P^{\sigma}$ in terms of $\overline{G}$ and $\tilde{\Sigma}^{\sigma}$. The method is described in Appendix C. We find

$$P^{\sigma}G^{\sigma}P^{\sigma}=\overline{X}[I+(\Sigma_1^{\sigma}-\Sigma_3^{\sigma}G_2\Sigma_3^{\sigma\dagger})\overline{X}+\Sigma_3^{\sigma}G_3^{\dagger}]^{-1}\,, \tag{3.16a}$$

where

$$\overline{X}=(I+G_3\Sigma_3^{\sigma\dagger})^{-1}G_1\,. \tag{3.16b}$$

In order to evaluate these expressions, we need to calculate three terms: Σ_1^{σ}, $G_3^{\sigma}\Sigma_3^{\dagger}$, and $\Sigma_3^{\sigma}G_2^{\sigma}\Sigma_3^{\sigma\dagger}$. Σ_1^{σ} is just a finite sum of finite matrices and can be evaluated directly. The other two terms involve sums which range over all sites in the solid and must be evaluated by Fourier transforms. We obtain

$$(G_3\Sigma_3^{\sigma\dagger})_{t,t'}=N^{-1}\sum_{\vec{q}}\overline{G}(\vec{q})\sum_{u,j}\sum_{r}e^{i\vec{q}\cdot\vec{R}_{tr}}M(\vec{q};u)^{\sigma j}_{r,t'-u}e^{-i\vec{q}\cdot\vec{R}_{u0}}-(G_1\Sigma_p^{\sigma\dagger})_{t,t'}, \tag{3.17a}$$

$$(\Sigma_3G_2\Sigma_3^{\sigma\dagger})_{t,t'}=N^{-1}\sum_{\vec{q}}\sum_{rr'}\sum_{u,j,u',j'}\overline{G}(\vec{q})e^{i\vec{q}\cdot\vec{R}_{uu'}}M^{\dagger}(\vec{q};u)^{\sigma j}_{t-u,r}e^{i\vec{q}\cdot\vec{R}_{rr'}}M(\vec{q};u')^{\sigma j'}_{r',t'-u'}$$
$$-(\Sigma_p^{\sigma}G_1\Sigma_p^{\sigma\dagger})_{t,t'}+(\Sigma_p^{\sigma}G_3\Sigma_3^{\sigma\dagger})_{t,t'}+(\Sigma_3^{\sigma}G_3^{\dagger}\Sigma_p^{\sigma\dagger})_{t,t'}, \tag{3.17b}$$

$$M(\vec{q};u)^{\sigma j}_{x,y}=\sum_{r,n}\sum_{i}K'^{\sigma_i}_{x,r}F(\vec{q})^{\sigma_i\sigma_j}_{r,n-u}K'^{\dagger\sigma_j}_{n-u,y}, \tag{3.17c}$$

where t, t', r, r' are sites onto which P^{σ} projects, $\sigma_j(u)\ U\sigma\in T$, $\sigma_{j'}(u')U\sigma\in T$, and for α, $\alpha'\in T$

$$\Sigma_p^{\sigma}=P^{\sigma}\Bigl(\sum_{\alpha U\sigma\in T}\sum_{\alpha'}K'^{\alpha}F^{\alpha\alpha'}K'^{\dagger\alpha'}\Bigr)P^{\sigma}\,. \tag{3.17d}$$

Σ_p^{σ}, like Σ_1^{σ}, can be evaluated directly.

In an effort to make these rather complicated equations less formidable, we describe the relation between this self-consistent approximation and the more familiar CPA. First rewrite $F(\vec{q})$ by combining Eqs. (3.11), (3.13), and (3.14), to obtain

$$F(\vec{q})^{\sigma\sigma'}_{mn}=\{G\{I-[\tilde{V}(\vec{q})-\tilde{\Sigma}]G\}^{-1}\}^{\sigma\sigma'}_{mn}, \tag{3.18}$$

where G is defined by $\langle if_{\sigma}|G|jf_{\sigma'}\rangle=G^{\sigma}_{ij}\delta^{\sigma\sigma'}$. If we define $\hat{V}=\hat{H}-\overline{H}\hat{I}$ by analogy with Eq. (2.16), and calculate the self-energy (3.10), then using the notation of Eq. (2.12)

$$0=-\Sigma(\vec{q})+\sum_{n,m}e^{i\vec{q}\cdot\vec{R}_{nm}}\{V'G\{I-[\tilde{V}(\vec{q})-\tilde{\Sigma}]G\}^{-1}V'^{\dagger}\}_{nm}\,. \tag{3.19}$$

In the CPA, the configuration-averaged t matrix is set equal to zero; i.e., $\langle(V-\Sigma)[1-(V-\Sigma)G]^{-1}\rangle_{\text{av}}=0$, which can be expressed as

$$0=\langle V-\Sigma\rangle_{\text{av}}+\langle(V-\Sigma)G[1-(V-\Sigma)G]^{-1}(V-\Sigma)\rangle_{\text{av}}\,. \tag{3.20}$$

Note that Eqs. (3.19) and (3.20) are similar in structure. In the CPA limit, where we have only diagonal disorder and single-site averages, (3.19) reduces to (3.20) since $\tilde{V}(\vec{q})$ is independent of $\vec{q}$. By comparison with the average t-matrix construction of the CPA [Eq. (3.20)], we can view the self-energy Eq. (3.19) [in the general disorder case when $\tilde{V}(\vec{q})$ is dependent on $\vec{q}$] as containing the analog of the t matrix for traveling clusters of excitations.

In the following two sections we use the self-consistent approximation for numerical calculations of the electronic and vibrational properties of disordered linear chains.

IV. ELECTRONS IN A ONE-DIMENSIONAL TIGHT-BINDING ALLOY

One of the most studied models in disordered systems is the one-dimensional, s-state, tight-binding, binary alloy with nearest-neighbor interactions,

$$H_{ij}=e(s_i)\delta_{ij}+W_{ij}(s_i,s_j)\,, \tag{4.1}$$

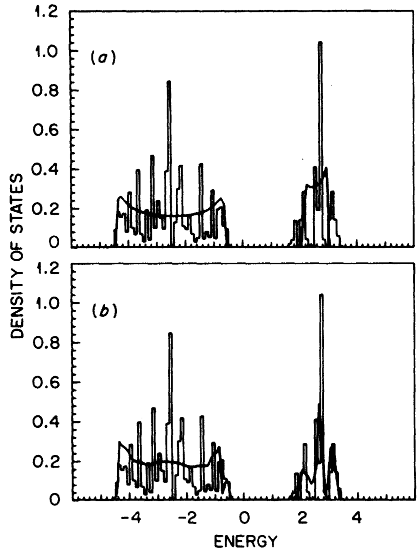

FIG. 4. Density of states for electrons in a linear chain with $e(A)=-e(B)=-2.5$, $W(A,A)=1.0$, $W(A,B)=W(B,B)=0.5$, and $c_B=0.3$. Comparison of the exact results (histogram) with the self-consistent (a) single-site and (b) nearest-neighbor pair approximations.

where $W_{ij}\neq 0$ when $j=i\pm 1$ and $s_i=A, B$ with probabilities c_A, c_B. We apply the self-consistent approximation described above for two cases, single-site scattering and nearest-neighbor pair scattering.

A. Single-site approximation

We let $T=\{\sigma \mid \sigma=\{i\}\ \forall i\}$ and $\sigma(0)=\{0\}$, where the sites of the linear chain are labeled consecutively. P^σ projects onto the sites $\{-1,0,1\}$ surrounding $\{0\}$ where $\tilde{V}$ is nonzero. The equations in Sec. III which define the self-consistent approximation are described in terms of three matrices: K'^σ, $\tilde{V}(q)$, and $\overline{K}$, whose values are given by

$$K'^{\sigma}_{ij}=\begin{cases}-e', & i=j=0\\ -H_2, & i=0,\ j=\pm 1;\ \ i=\pm 1,\ j=0\\ 0, & \text{otherwise}\end{cases} \tag{4.2}$$

$$\tilde{V}(q)^{\sigma,\sigma}_{ij}=\begin{cases}(\tilde{e}-\overline{e})+2H_3\cos q, & i=j=0\\ H_4-H_1, & i=0,\ \ j=\pm 1;\ \ i=\pm 1,\ j=0\\ H_3 e^{iq}, & i=1,\ j=-1\\ H_3 e^{-iq}, & i=-1,\ j=1\\ 0, & \text{otherwise}\end{cases} \tag{4.3}$$

and

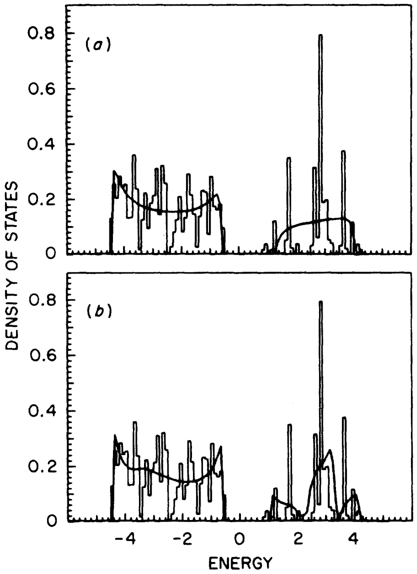

FIG. 5. Density of states for electrons in a linear chain in the diagonal disorder limit; $e(A)=-e(B)=-2.5$, $W(A,A)=W(A,B)=W(B,B)=1.0$, and $c_B=0.3$. Comparison of the exact results (histogram) with the self-consistent (a) single-site and (b) nearest-neighbor pair approximations.

$$\overline{K}_{ij}=\begin{cases}z-\overline{e}, & i=j\\ -H_1, & i=j\pm 1\\ 0, & \text{otherwise}\end{cases} \tag{4.4}$$

where

$$\begin{aligned}
\overline{e}&=c_A e(A)+c_B e(B)\,,\\
\tilde{e}&=c_B e(A)+c_A e(B)\,,\\
e'&=(c_A c_B)^{1/2}[e(A)-e(B)]\,,\\
H_1&=c_A^2 W(A,A)+2c_A c_B W(A,B)+c_B^2 W(B,B)\,,\\
H_2&=(c_A c_B)^{1/2}[c_A W(A,A)+(c_B-c_A)W(A,B)\\
&\qquad -c_B W(B,B)]\,,\\
H_3&=c_A c_B[W(A,A)-2W(A,B)+W(B,B)]\,,\\
H_4&=c_A c_B[W(A,A)+W(B,B)]+(c_A^2+c_B^2)W(A,B)\,.
\end{aligned} \tag{4.5}$$

(We have chosen the lattice spacing to be 1 in these examples.) Even though we consider only a single excitation, the effects of the neighbors are included explicitly through the off-diagonal terms H_1, H_2, H_3, and H_4.

In Fig. 4(a) we compare the densities of states evaluated with the self-consistent, single-site approximation with the essentially exact results obtained by node counting[22] for linear chains of 10 000 atoms with $e(A)=-e(B)=-2.5$, $W(A,A)=1.0$, $W(A,B)=W(B,B)=0.5$ and $c_B=0.3$. The single-site approximation produces a smooth distribution which predicts the band edges of the host band centered at −2.5 quite accurately. For the defect band the approximation results in a distribution which underestimates the bandwidth, but which is centered properly about the major defect band peaks. Since this calculation is a single-site approximation, we do not pick up any of the detailed peak structure in the bands.

For completeness we have included in Fig. 5(a) a calculation for the limiting case of diagonal disorder where this self-consistent approximation reduces to the CPA. Here $e(A)=-e(B)=-2.5$, $W(A,A)=W(A,B)=W(B,B)=1$, and $c_B=0.3$. Note that in the defect band the self-consistent approximation gives a somewhat better estimate of the bandwidth for diagonal disorder. We expect to see a marked improvement in the defect bands when we apply the self-consistent pair approximation below.

B. Pair approximation

In the pair approximation we include single-site and nearest-neighbor pair scattering. $T=\{\sigma \mid \sigma_1=\{i\}, \sigma_2=\{i,i+1\} \forall \text{ sites } i\}$ and $\sigma_1(0)=\{0\}$, $\sigma_2(0)=\{0,1\}$. In this case, P^{σ_1} projects onto sites $\{-2,-1,0,1,2\}$ and P^{σ_2} projects onto $\{-1,0,1,2\}$. The matrix equations become somewhat more complex than those for the single-site case above. K'^{σ_1} and $\tilde{V}(q)^{\sigma_1,\sigma_1}$ are identical to K'^{σ} and $\tilde{V}^{\sigma,\sigma}$ defined for the single-site case in Eqs. (4.2) and (4.3) above, respectively. In addition, we find

$$K'^{\sigma_2}_{ij}=\begin{cases}-H_3, & i=0,\ j=1;\ i=1,\ j=0\\ 0, & \text{otherwise}\end{cases} \tag{4.6}$$

$$\tilde{V}(q)^{\sigma_2,\sigma_2}_{ij}=\begin{cases}\tilde{e}-\bar{e}, & i=j=0,1\\ H_4-H_1, & i=0,\ j=-1;\ \ i=-1,\ j=0;\ \ i=1,\ j=2;\ \ i=2,\ j=1\\ H_5-H_1, & i=1,\ j=0;\ \ i=0,\ j=1\\ 0, & \text{otherwise}\end{cases} \tag{4.7}$$

$$\tilde{V}(q)^{\sigma_1\sigma_2}_{ij}=\begin{cases}e', & i=j=1\\ H_6, & i=1,\ j=0;\ \ i=0,\ j=1\\ H_2, & i=1,\ j=2;\ \ i=2,\ j=1\\ e'e^{-iq}, & i=-1,\ j=0\\ H_5e^{-iq}, & i=0,\ j=0;\ \ i=-1,\ j=1\\ H_2e^{-iq}, & i=-1,\ j=-1;\ \ i=2,\ j=0\\ 0, & \text{otherwise}\end{cases} \tag{4.8}$$

and

$$\tilde{V}(q)^{\sigma_2\sigma_1}_{ij}=\tilde{V}^*(q)^{\sigma_1\sigma_2}_{ji}, \tag{4.9}$$

where

$$\begin{aligned}H_5&=c_B^2W(A,A)+2c_Ac_BW(A,B)+c_A^2W(B,B),\\ H_6&=(c_Ac_B)^{1/2}[c_BW(A,A)+(c_A-c_B)W(A,B)-c_AW(B,B)].\end{aligned} \tag{4.10}$$

As anticipated, the change from a single-site to a pair approximation produces a significant improvement in the density of states generated by the self-consistent approximation. For the off-diagonal disorder example above, we find that not only does the self-consistent theory give excellent estimates of the bandwidths in both host and defect bands, but a distinctive three-peaked structure has appeared in the defect band which closely matches the major peaks in the exact results [see Fig. 4(b)]. As noted by Dean,[22] the central peak in the defect band corresponds primarily to states localized on isolated B atoms and the two satellite peaks correspond primarily to bonding and antibonding states localized on B-B pairs. Furthermore, there is some smaller structure which appears in the host band due to A-A and A-B pairs.

The pair approximation produces similar results for the diagonal disorder example shown in

Fig. 5(b). As we mentioned earlier, the diagonal disorder limit of our self-consistent approximation is the traveling cluster approximation of Mills and Ratanavararaksa.[11]

Of course, in order to reproduce all of the spikes in the very ragged one-dimensional density of states it is necessary to include larger clusters in the approximation. In higher dimensions, the contributions from large clusters are considerably less important since each atom has many more neighbors. Thus, the atoms are in a more nearly average environment, and the density of states is smoother.

V. PHONONS IN A DISORDERED HARMONIC LINEAR CHAIN

In Sec. IV we examined a tight-binding system with diagonal and off-diagonal disorder. In this Section we calculate the frequency spectrum for a system with environmental disorder as well. The inverse of the Green's function for a binary, harmonic, linear mixed crystal with nearest-neighbor forces can be written as

$$G^{-1}_{ij}=\left(m(s_i)\omega^2-\sum_{l\neq i}\phi_{il}(s_i,s_l)\right)\delta_{ij}+\phi_{ij}(s_i,s_j)\,, \tag{5.1}$$

where $m(s_i)$ is the mass of the atom at site i, the spring constant $\phi_{ij}\neq 0$ when $j=i\pm 1$, and $s_i=A, B$ with probabilities c_A, c_B. [The force constant matrix Φ is equal to the negative of the sum of the last two terms on the right in Eq. (5.1).] The environmental disorder appears in the second term on the right-hand side of Eq. (5.1). As a result of this term, the diagonal element G^{-1}_{ii} depends on the occupation of neighboring sites. Since the density of states in a phonon system is derived from the average of the operator MG rather than G, we have included a brief description of the calculation of this quantity using augmented-space methods in Appendix D.

We consider two cases, just as we did in Sec. IV for the electronic problem.

A. Single-site approximation

We choose T as above, namely, $T=\{\sigma\,|\,\sigma=\{i\}\;\forall\, i\}$ and $\sigma(0)=\{0\}$. Thus, we find

$$K'^{\sigma}_{ij}=\begin{cases}u'\omega^2-2D_2, & i=j=0\\ D_2, & i=0,\ j=\pm 1;\ \ i=\pm 1,\ j=0\\ -D_2, & i=j=\pm 1\\ 0, & \text{otherwise}\end{cases} \tag{5.2}$$

$$\tilde{V}(q)^{\sigma,\sigma}_{ij}=\begin{cases}(\bar{u}-\tilde{u})\omega^2-2(D_1-D_4)-2D_3\cos q, & i=j=0\\ (D_1-D_4)+D_3e^{-iq}, & i=-1,\ j=0;\ \ i=0,\ j=1\\ \tilde{V}^{*}_{ji}, & i=0,\ j=-1;\ \ i=1,\ j=0\\ -D_3e^{-iq}, & i=-1,\ j=1\\ \tilde{V}^{*}_{ji}, & i=1,\ j=-1\\ D_4-D_1, & i=j=\pm 1\\ 0, & \text{otherwise}\end{cases} \tag{5.3}$$

$$\overline{V}_{ij}=\begin{cases}\bar{u}\omega^2-2H_1, & i=j\\ H_1, & i=j\pm 1\\ 0, & \text{otherwise}\end{cases} \tag{5.4}$$

where

$$\begin{aligned}
&\bar{u}=c_A m(A)+c_B m(B)\,,\\
&\tilde{u}=c_B m(A)+c_A m(B)\,,\\
&u'=(c_A c_B)^{1/2}[m(A)-m(B)]\,,\\
&D_1=c_A^2\phi(A,A)+2c_A c_B\phi(A,B)+c_B^2\phi(B,B)\,,\\
&D_2=(c_A c_B)^{1/2}[c_A\phi(A,A)+(c_B-c_A)\phi(A,B)-c_B\phi(B,B)]\,,\\
&D_3=c_A c_B[\phi(A,A)-2\phi(A,B)]+\phi(B,B)\,,\\
&D_4=c_A c_B[\phi(A,A)+\phi(B,B)]+(c_A^2+c_B^2)\phi(A,B)\,.
\end{aligned} \tag{5.5}$$

In Fig. 6(a) we compare the densities of states evaluated with the self-consistent, single-site approximation with the essentially exact results obtained by node counting[22] for a linear chain of 10 000 atoms with $m(A)=1.0$, $m(B)=0.5$, $\phi(A,A)=1.0$, $\phi(A,B)=1.25$, $\phi(B,B)=0.75$, and $c_B=0.25$. The frequency spectrum of the single-site approximation is relatively smooth. It misses the remnant of the perfect A crystal singularity near $\omega^2=4$ and has a tail in the high-frequency region just above where the exact results cut off. However, it does give a good overall estimate of the density of states. Of course, none of the detailed structure within the bands appears in the single-site approximation.

B. Pair approximation

Again we choose T as we did for the electron problem $T=\{\sigma\,|\,\sigma_1=\{i\},\ \sigma_2=\{i,i+1\}\ \forall\ i\}$ and $\sigma_1(0)=\{0\}$, $\sigma_2(0)=\{0,1\}$. The projection operators are the same as before, P^{σ_1} projects onto sites $\{-2,-1,0,1,2\}$ and P^{σ_2} projects onto $\{-1,0,1,2\}$. We find that $K'^{\sigma_1}=K'^{\sigma}$ and $\tilde{V}^{\sigma_1,\sigma_1}=\tilde{V}^{\sigma,\sigma}$ which are defined in (5.2) and (5.3), respectively. In addition we have

$$K'^{\sigma_2}_{ij}=\begin{cases}-D_3, & i=j=0,1\\ D_3, & i=0,\ j=1;\ \ i=1,\ j=0\\ 0, & \text{otherwise}\end{cases} \tag{5.6}$$

$$\tilde{V}(q)^{\sigma_2,\sigma_2}_{ij}=\begin{cases}(\bar{u}-\tilde{u})\omega^2-2D_1+D_5+D_4, & i=0,\ j=0;\ \ i=1,\ j=1\\ D_1-D_4, & i=-1,\ j=0;\ \ i=0,\ j=-1;\ \ i=1,\ j=2;\ \ i=2,\ j=1\\ D_4-D_1, & i=j=-1,2\\ D_1-D_4, & i=0,\ j=1;\ \ i=1,\ j=0\\ 0, & \text{otherwise,}\end{cases} \tag{5.7}$$

$$\tilde{V}(q)^{\sigma_1,\sigma_2}_{ij}=\begin{cases}(-u'\omega^2+D_1+D_6)e^{-iq}, & i=-1,\ j=0\\ D_6(1-e^{-iq}), & i=j=0\\ D_6(e^{-iq}-1), & i=0,\ j=1\\ -D_6e^{-iq}, & i=-1,\ j=1\\ -u'\omega^2+D_2+D_6, & i=j=1\\ -D_2e^{-iq}, & i=j=-1;\ \ i=-2,\ j=0\\ D_2e^{-iq}, & i=-2,\ j=-1\\ -D_6, & i=1,\ j=0\\ -D_2, & i=1,\ j=2;\ \ i=2,\ j=1\\ 0, & \text{otherwise}\end{cases} \tag{5.8}$$

$$\tilde{V}(q)^{\sigma_2,\sigma_1}_{ij}=\tilde{V}^*(q)^{\sigma_1,\sigma_2}_{ji}\,, \tag{5.9}$$

where

$$\begin{aligned}
&D_5=c_B^2\phi(A,A)+2c_A c_B\phi(A,B)+c_A^2\phi(B,B)\,,\\
&D_6=(c_A c_B)^{1/2}[c_A\phi(A,A)+(c_B-c_A)\phi(A,B)-c_A\phi(B,B)]\,.
\end{aligned} \tag{5.10}$$

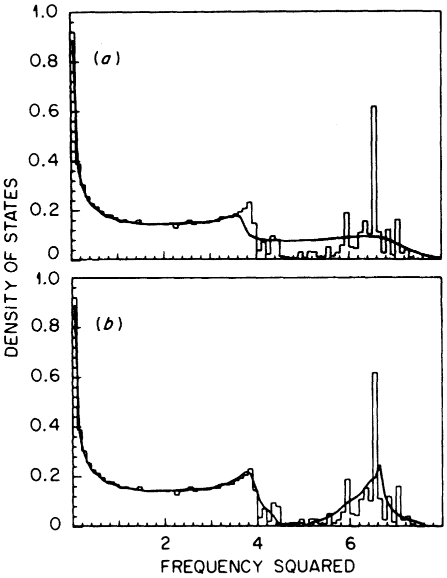

FIG. 6. Density of states for phonons in a harmonic linear chain with $m(A)=1.0$, $m(B)=0.5$, $\phi(A,A)=1.0$, $\phi(A,B)=1.25$, $\phi(B,B)=0.75$, and $c_B=0.25$. Comparison of the exact results (histogram) with the self-consistent (a) single-site and (b) nearest-neighbor pair approximations.

Once again the change from a single-site to a pair approximation produces significant improvements in the frequency spectrum generated by the self-consistent approximation. We see in Fig. 6(b) that the pair approximation exhibits the structure associated with the perfect A crystal band edge near $\omega^2=4$ and that the tailing at high frequencies is reduced, giving a good estimate of the high-frequency band edge. Furthermore, we now see the major structure within the defect band. There is a dominant peak at high frequencies which is centered near the isolated B atom modes. In addition there are shoulders to either side of the central peak and one just above the structure at $\omega^2=4$ as well as a small bump near $\omega^2=5$ which result from B-B and A-B pairs. The host band remains relatively structureless and the frequency spectrum approaches the virtual-crystal limit as the frequency becomes small.

VI. CONCLUSION

We have presented a self-consistent cluster theory for elementary excitations in random substitutional alloys with diagonal, off-diagonal, and environmental disorder. In this theory a systematic set of approximations for the self-energy are developed in terms of an operator formalism, and illustrated by diagrams. The approximate configuration-averaged Green's function has the proper translational symmetry and is proved to be analytic. This theory is a natural generalization of the diagonal disorder approximation of Mills and Ratanavararaksa[11] to the more general problem of off-diagonal and environmental disorder. Example calculations for single-site and pair approximations for the one-dimensional electron and phonon densities of states show good agreement with exact results and demonstrate the marked improvement which results from the inclusion of pair scattering. In three dimensions we expect significantly better agreement since much of the structure in the exact density of states tends to disappear, as each atom sees a more nearly average environment. A comparison of the diagonal disorder one-dimensional example presented in Fig. 5 with the three-dimensional examples presented by Mills and Ratanavararaksa[11] provides a clear demonstration of this point.

This theory exhibits the proper behavior in all physical limits (dilute, weak scattering, and strong scattering). In particular, in the dilute limit for nearest-neighbor interactions we note that the approximation reduces to a $(Z+1)\times(Z+1)$ matrix theory which appropriately gives all the localized states about a single defect. Furthermore, since this theory is applicable to general disorder problems, physical effects such as lattice relaxation about defects and charge transfer (which give rise to off-diagonal and environmental disorder) can be treated when the appropriate Hamiltonians are known.

There as yet remains one important restriction on this theory. It is not yet clear how to apply this approximation to disordered systems with short-range order (dependent random variables). This is despite the fact that short-range order can be represented in augmented space.[14] The nontranslationally invariant form of the augmented-space operators for short-range order, as presented in Ref. 14, invalidates the Fourier-transform procedure used to solve the self-consistent equations.

The theory appears quite complicated as a matrix theory in $\vec{q}$ space. However, this complication is essential for properly including cluster scattering in general disorder problems.

ACKNOWLEDGMENTS

The authors are grateful to R. L. Mills for helpful conversations and for a copy of Ref. 11 in advance of publication. This research was sponsored by the Division of Materials Sciences, U. S. Department of Energy under Contract No. W-7405-eng-26 with the Union Carbide Corporation. Two of us (H. W. D. and P. L. L.) are grateful to the Solid State Division of Oak Ridge National Laboratory for its hospitality when this work was begun; we also gratefully acknowledge partial support for this work by the National Science Foundation through Grant No. DMR78-10813. One of us (H. W. D.) would also like to thank the German Academic Exchange Service (DAAD) for its support with a NATO fellowship.

APPENDIX A: PROOF OF ANALYTICITY

Using an argument similar to that in Ref. 11, we will demonstrate that, subject to a few mild conditions, the self-consistent equations developed in Sec. III have a unique solution, and that this solution yields a Herglotz Green's function. Recall that the operator-valued function $F(z)$ is called Herglotz provided $F(z)$ is analytic in the cut plane $\mathrm{Im}z \neq 0$, $F(z^*) = F^\dagger(z)$, and

$$\mathrm{Im}F(z) = (1/2i)[F(z) - F^\dagger(z)] \leq 0$$

for all z in the upper half plane.

In the notation of Secs. II and III, $\Omega = \Psi \otimes \Theta$ is the augmented Hilbert space, Ψ is the real space on which the random Hamiltonian H acts, and Θ is the disorder space. The space Θ is a direct product $\prod \theta_l$, where l runs over the index set of the random variables $\{s_l\}$, and we refer to θ_l as site l. A basis for Θ consists of the ground-state vector $|f\rangle$, together with vectors of the form $|f_\sigma\rangle$, where σ represents a collection of sites which are in the excited state (for multicomponent systems, σ would also specify which excited state was present at each site). The projection onto the subspace $\Psi \otimes |f_\sigma\rangle$ will be denoted by P_σ, and, as customary, when σ is the null set we drop the subscript. Thus P is the projection onto $\Psi \otimes |f\rangle$. If T is the collection of sets which defines the self-consistent approximation (in Mills's notation, the family of overlap sets), we set $P_T = \sum_{\sigma \in T} P_\sigma$. Any real-space operator $X:\Psi \to \Psi$ can be enlarged to an augmented-space operator $\hat{X}$ by defining $\hat{X} = X \otimes 1_\Theta$. If, for each $\sigma \in T$, there is a real-space operator X^σ, we define $\{X^\sigma\}_T \equiv \sum_{\sigma \in T} \hat{X}^\sigma P_\sigma$. For example, if $X^\sigma = 1_\Psi$ for all σ, then $\{X^\sigma\}_T = P_T$.

From Eqs. (2.11)–(2.16), the configuration-averaged Green's function is given by $\bar{G} = (G_{\mathrm{vc}}^{-1} - \Sigma)^{-1}$ and the self-energy $\Sigma = K'FK'^\dagger$. In the T approximation [Eq. (3.3)],

$$F = [\{(G^\sigma)^{-1}\}_T - P_T \tilde{V} P_T]^{-1} , \tag{A1}$$

where $\tilde{V}$ is the augmented-space potential defined by Eq. (2.16), $\sigma \in T$, and

$$G^\sigma = (\bar{G}^{-1} + \tilde{\Sigma}^\sigma)^{-1} \tag{A2}$$

with

$$\tilde{\Sigma}^\sigma = \Sigma - \Sigma^\sigma = \sum_{\alpha \cup \sigma \in T, \text{ or } \alpha' \cup \sigma \in T} K'^\alpha F^{\alpha\alpha'} K'^{\dagger\alpha'} . \tag{A3}$$

In the above equation, and in the following, α and α' will denote sets of sites that belong to T. From the definition (A2), we see that

$$G^\sigma = (G_{\mathrm{vc}}^{-1} - \Sigma + \tilde{\Sigma}^\sigma)^{-1} = (G_{\mathrm{vc}}^{-1} - \Sigma^\sigma)^{-1} \tag{A4}$$

and thus, substituting from Eqs. (A1) and (A3) we find that

$$G^\sigma = \left(G_{\mathrm{vc}}^{-1} - \sum_{\alpha \cup \sigma \notin T, \ \alpha' \cup \sigma \notin T} K'^\alpha [\{(G^\sigma)^{-1}\}_T - P_T \tilde{V} P_T]^{-1\alpha\alpha'} K'^{\dagger\alpha'}\right)^{-1} . \tag{A5}$$

If we denote by $P_{T,\sigma}$ the projection $\sum_{\alpha \cup \sigma \notin T} P_\alpha$, Eqs. (A5) and (A4) become

$$G^\sigma = (G_{\mathrm{vc}}^{-1} - K'P_{T,\sigma}[\{(G^\sigma)^{-1}\}_T - P_T \tilde{V} P_T]^{-1} P_{T,\sigma} K'^\dagger)^{-1} \tag{A6}$$

and

$$\Sigma^\sigma = G_{\mathrm{vc}}^{-1} - (G^\sigma)^{-1} = K'P_{T,\sigma}[\{(G^\sigma)^{-1}\}_T - P_T \tilde{V} P_T]^{-1} P_{T,\sigma} K'^\dagger . \tag{A7}$$

Summing Eq. (A7) over σ we finally obtain

$$\{\Sigma^\sigma\}_T = \{K'P_{T,\sigma}[\{(G^\sigma)^{-1}\}_T - P_T \tilde{V} P_T]^{-1} P_{T,\sigma} K'^\dagger\}_T \equiv \mathfrak{F}(\{\Sigma^\sigma\}_T) . \tag{A8}$$

By virtue of its dependence on G^σ and Eq. (A4), $\mathfrak{F}$ is a function of $\{\Sigma^\sigma\}_T$ and E, and our task is to show that $\mathfrak{F}$ has a unique fixed point $\{\Sigma^\sigma\}_T$ for each E, and that this in turn yields a Herglotz Green's function $\bar{G}$. By suitably restricting the range of E and $\{\Sigma^\sigma\}_T$, we can show that $\mathfrak{F}$ maps a certain (complete metric) space into itself. Iterating Eq. (A8) will yield a Cauchy sequence which converges to the required fixed point.

We make the following assumptions. The variable E is restricted to a compact subset R of the upper half plane, and on R, $-G_{\mathrm{vc}}^{-1}(E)$ is a Herglotz function. Furthermore, for any $E \in R$, $\mathrm{Im}G_{\mathrm{vc}}^{-1}$ is uniformly bounded away from 0; i.e., $\mathrm{Im}G_{\mathrm{vc}}^{-1}(E) \geq y > 0$. For simplicity, we also assume that $\bar{G} = \langle (G_{\mathrm{vc}}^{-1} - A)^{-1} \rangle$, where A is Hermitian and independent of E; thus $\tilde{V}$ is Hermitian, while K' and $K'^\dagger$ are Hermitian conjugates. This assumption is true for the electronic problem, but not for the phonon problem. However, for the phonon problem, a simple argument involving operator MG can be used to reduce this problem to the situation considered here. Finally, we assume that $\tilde{V}$ and K' are bounded operators.

We begin the proof by showing that the imaginary part of $\mathfrak{F}(\{\Sigma^\sigma\}_T)$ is negative definite:

$$
\begin{aligned}
\mathrm{Im}\,\mathfrak{F}(\{\Sigma^\sigma\}_T) &= (1/2i)[\mathfrak{F}(\{\Sigma^\sigma\}_T) - \mathfrak{F}(\{\Sigma^\sigma\}_T)^\dagger] \\
&= (1/2i)(\{K'P_{T,\sigma}[\{(G^\sigma)^{-1}\}_T - P_T\tilde{V}P_T]^{-1}P_{T,\sigma}K'^\dagger\}_T - \{K'P_{T,\sigma}[\{(G^\sigma)^{-1}\}_T^\dagger - P_T\tilde{V}P_T]^{-1}P_{T,\sigma}K'^\dagger\}_T) \\
&= \{K'P_{T,\sigma}[\{(G^\sigma)^{-1}\}_T - P_T\tilde{V}P_T]^{-1}\{-\mathrm{Im}(G^\sigma)^{-1}\}_T[\{(G^\sigma)^{-1}\}_T^\dagger - P_T\tilde{V}P_T]^{-1}P_{T,\sigma}K'^\dagger\}_T\,.
\end{aligned}
\tag{A9}
$$

However, $-\mathrm{Im}(G^\sigma)^{-1} = \mathrm{Im}\Sigma^\sigma - \mathrm{Im}G_{\mathrm{vc}}^{-1}$, and since $\mathrm{Im}G_{\mathrm{vc}}^{-1} \geqslant y > 0$, we see that $-\mathrm{Im}(G^\sigma)^{-1} < 0$ whenever $\mathrm{Im}\Sigma^\sigma \leqslant 0$. Thus, if $\{\Sigma^\sigma\}_T^1$ has a negative definite imaginary part, iteration of the equation $\{\Sigma^\sigma\}_T^{j+1} = \mathfrak{F}(\{\Sigma^\sigma\}_T^j)$ always maintains this property. From $\mathrm{Im}G_{\mathrm{vc}}^{-1} \geqslant y > 0$ it also follows that $\mathfrak{F}(\{\Sigma^\sigma\}_T)$ is bounded:

$$
\begin{aligned}
\|\mathfrak{F}(\{\Sigma^\sigma\}_T)\| &= \|\{K'P_{T,\sigma}[\{(G^\sigma)^{-1}\}_T - P_T\tilde{V}P_T]^{-1}P_{T,\sigma}K'^\dagger\}_T\| \\
&\leqslant \sup_{\sigma\in T}\|K'\|\;\|K'^\dagger\|\;\|[\{(G^\sigma)^{-1}\}_T - P_T\tilde{V}P_T]^{-1}\|\,,
\end{aligned}
\tag{A10}
$$

and using (A4)

$$\mathrm{Im}[\{(G^\sigma)^{-1}\}_T - P_T\tilde{V}P_T] = \{\mathrm{Im}G_{\mathrm{vc}}^{-1} - \mathrm{Im}\Sigma^\sigma\}_T \geqslant y\,.$$

This implies $\|[\{(G^\sigma)^{-1}\}_T - P_T\tilde{V}P_T]^{-1}\| \leqslant 1/y$ and hence,

$$\|\mathfrak{F}(\{\Sigma^\sigma\}_T)\| \leqslant \gamma\,, \tag{A11}$$

where $\gamma = \|K'\|^2/y$. If we define the set of augmented-space operators D by

$$D = \{X \mid X = \{X^\sigma\}_T,\ \mathrm{Im}X^\sigma < 0,\ \|X^\sigma\| \leqslant \gamma\}\,, \tag{A12}$$

then we can summarize the above results as showing that $\mathfrak{F}: D \to D$.

We next prove that the sequence $\{\Sigma^\sigma\}_T^{n+1} = \mathfrak{F}(\{\Sigma^\sigma\}_T^n)$ is a Cauchy sequence. Let $\Delta\Sigma_n = \{\Sigma^\sigma\}_T^{n+1} - \{\Sigma^\sigma\}_T^n$; then

$$
\begin{aligned}
\Delta\Sigma_n &= \mathfrak{F}(\{\Sigma^\sigma\}_T^n) - \mathfrak{F}(\{\Sigma^\sigma\}_T^{n-1}) \\
&= \{K'P_{T,\sigma}[\{(G^\sigma)^{-1}\}_T^n - P_T\tilde{V}P_T]^{-1}\Delta\Sigma_{n-1}[\{(G^\sigma)^{-1}\}_T^{n-1} - P_T\tilde{V}P_T]^{-1}P_{T,\sigma}K'^\dagger\}_T\,.
\end{aligned}
\tag{A13}
$$

Let $g_n = \mathrm{Im}[\{(G^\sigma)^{-1}\}_T^n - P_T\tilde{V}P_T] = \mathrm{Im}\hat{G}_{\mathrm{vc}}^{-1}P_T - \mathrm{Im}\{\Sigma^\sigma\}_T^n \geqslant y$. Since g_n is positive definite, there is a positive-definite square root $\sqrt{g_n}$, and we have

$$\Delta\Sigma_n = \left\{Y_n^{\sigma\dagger}\frac{1}{\sqrt{g_n}}\Delta\Sigma_{n-1}\frac{1}{\sqrt{g_{n-1}}}Y_{n-1}^\sigma\right\}_T\,, \tag{A14a}$$

where

$$Y_n^\sigma = \sqrt{g_n}\,[\{(G^\sigma)^{-1}\}_T^n - P_T\tilde{V}P_T]^{-1}P_{T,\sigma}K'^\dagger\,. \tag{A14b}$$

Let $Y_n^\sigma = W_n^\sigma J_n^\sigma$ be the polar decomposition[23] of Y_n^σ; $J_n = (Y_n^{\sigma\dagger}Y_n^\sigma)^{1/2}$ and W_n^σ is a partial isometry from the range of J_n^σ (= range of $Y_n^{\sigma\dagger} \subset P$) to the range of Y_n^σ. Since J_n^σ maps P into P, (A14a) becomes

$$\Delta\Sigma_n = \{J_n^\sigma\}_T\left\{W_n^{\sigma\dagger}\frac{1}{\sqrt{g_n}}\Delta\Sigma_{n-1}\frac{1}{\sqrt{g_{n-1}}}W_{n-1}^\sigma\right\}_T\{J_{n-1}^\sigma\}_T\,. \tag{A15}$$

By defining $X_n = \{J_n^\sigma\}_T$ and

$$A_n = \left\{W_n^{\sigma\dagger}\frac{1}{\sqrt{g_n}}\Delta\Sigma_{n-1}\frac{1}{\sqrt{g_{n-1}}}W_{n-1}^\sigma\right\}_T\,, \tag{A16}$$

we can write (A15) as $\Delta\Sigma_n = X_nA_nX_{n-1}$, and substituting this back into (A16) we find

$$A_n = \left\{W_n^{\sigma\dagger}\frac{1}{\sqrt{g_n}}X_{n-1}A_{n-1}X_{n-2}\frac{1}{\sqrt{g_{n-1}}}W_{n-1}^\sigma\right\}_T\,. \tag{A17}$$

We will use (A17) to obtain an estimate of $\|A_n\|$ in terms of $\|A_{n-1}\|$. Since $\|W_n^\sigma\| = 1$, it follows that, for an arbitrary $\sigma \in T$

$$
\begin{aligned}
\left\|X_{n-1}\frac{1}{\sqrt{g_n}}W_n^\sigma\right\|^2 &\leqslant \left\|X_{n-1}\frac{1}{\sqrt{g_n}}\right\|^2 \\
&= \sup_\xi\left\langle\xi\left|\frac{1}{\sqrt{g_n}}X_{n-1}^\dagger X_{n-1}\frac{1}{\sqrt{g_n}}\right|\xi\right\rangle\Big/\|\xi\|^2\,,
\end{aligned}
\tag{A18}
$$

where $\xi \in P_T$, $\xi \neq 0$. Furthermore, using (A14b) and (A9)

$$X_n^\dagger X_n = \{(J_n^\sigma)^2\}_T = \{Y_n^{\sigma\dagger}Y_n^\sigma\}_T = -\mathrm{Im}\{\Sigma^\sigma\}_T^{n+1}\,. \tag{A19}$$

With the substitution $\chi = (1/\sqrt{g_n})\xi$, we find

$$
\begin{aligned}
\left\|X_{n-1}\frac{1}{\sqrt{g_n}}W_n^\sigma\right\|^2 &\leqslant -\sup_\xi\left\langle\xi\left|\mathrm{Im}\{\Sigma^\sigma\}_T^n\frac{1}{\sqrt{g_n}}\right|\xi\right\rangle\Big/\|\xi\|^2 \\
&\leqslant \sup_\chi\langle\chi|-\mathrm{Im}\{\Sigma^\sigma\}_T^n|\chi\rangle/\langle\chi|g_n|\chi\rangle \\
&\leqslant \sup_\chi\langle\chi|-\mathrm{Im}\{\Sigma^\sigma\}_T^n|\chi\rangle/(y + \langle\chi|-\mathrm{Im}\{\Sigma^\sigma\}_T^n|\chi\rangle)\,.
\end{aligned}
\tag{A20}
$$

This last expression is of the form $x/(y+x)$, $x>0$, whose maximum occurs on the boundary. Since $x \leq \|\mathrm{Im}\{\Sigma^\sigma\}_T^n\| \leq \gamma$, we have

$$\left\| X_{n-1} \frac{1}{\sqrt{g_n}} W_n \right\|^2 \leq \gamma/(y+\gamma) = \lambda < 1 . \tag{A21}$$

Thus, from (A17) $\|A_n\| \leq \lambda \|A_{n-1}\|$ and $\|A_n\| \leq \lambda^{n-1}\|A_1\|$. Furthermore,

$$\|\Delta\Sigma_n\| \leq \|X_n\| \; \|A_n\| \; \|X_{n-1}\| \leq \gamma \|A_n\| \leq \gamma\lambda^{n-1}\|A_1\| . \tag{A22}$$

It now follows immediately that $\{\Sigma^\sigma\}_T^n$ is a Cauchy sequence:

$$\|\{\Sigma^\sigma\}_T^n - \{\Sigma^\sigma\}_T^m\| = \left\| \sum_{j=m}^{n-1} \Delta\Sigma_j \right\| \leq \gamma \|A_1\| \sum_{m}^{n-1} \lambda^{j-1} \rightarrow 0 , \tag{A23}$$

as m and $n \rightarrow \infty$. Since the set of operators D is a closed set, $\{\Sigma^\sigma\}_T^n$ converges to a solution of the equation $\mathfrak{F}(X) = X$, and this solution also belongs to D. To verify that this is the only solution, assume that $\mathfrak{F}(Y) = Y$. Then, following the same line of reasoning as above for $X-Y = \mathfrak{F}(X) - \mathfrak{F}(Y)$, it is easy to show that $\|X - Y\| = 0$, or that $X = Y$.

It only remains to show that this solution $\{\Sigma^\sigma\}_T$ yields a Herglotz $\overline{G}$. Assuming $\{\Sigma^\sigma\}_T^1$ is an analytic function of E, each succeeding term $\{\Sigma^\sigma\}_T^n$ is analytic, and therefore the uniform limit (note that λ and γ are independent of E) $\{\Sigma^\sigma\}_T$ is also analytic. Finally,

$$\mathrm{Im}\Sigma(E) = K' \,\mathrm{Im} F K'^\dagger , \tag{A24}$$

and

$$\begin{aligned} \mathrm{Im}F &= [\{(G^\sigma)^{-1}\}_T - P_T \tilde{V} P_T]^{-1}[-\{\mathrm{Im}(G^\sigma)^{-1}\}_T][\{(G^\sigma)^{-1}\}_T^\dagger - P_T \tilde{V} P_T]^{-1} \\ &= [\{(G^\sigma)^{-1}\}_T - P_T \tilde{V} P_T]^{-1}\{\mathrm{Im}\Sigma^\sigma\}_T[\{(G^\sigma)^{-1}\}_T^\dagger - P_T \tilde{V} P_T]^{-1} , \end{aligned} \tag{A25}$$

and thus, $\mathrm{Im}F < 0$.

APPENDIX B: DIAGRAM SYMMETRY RULE

Ever since the appearance of the article of Nickel and Butler,[8] the analyticity or Herglotz nature of the approximate Green's function has been a key test for any theory. For approximations derived from a partial summation of diagrams, a better understanding of this question was provided by Mills and Ratanavararaksa[11] (which followed an unpublished work of Mills). By introducing a symmetry rule, they were able to guarantee that $\mathrm{Im}\Sigma$ is negative definite. The analyticity of the approximate Green's function defined herein is proved in Appendix A, but the essential feature that allows this proof to go through is the symmetry, imposed in accordance with Mills's rule, of the diagrams that are summed [Eq. (A6)]. Mills's symmetry rule was derived essentially as follows.

First, we consider the perturbation expansion of self-energy Σ obtained from Eqs. (2.19) and (2.20). The crux of the argument is a clever rewriting of the terms of $\mathrm{Im}\Sigma = (1/2i)(\Sigma - \Sigma^\dagger)$. The self-energy is a sum of irreducible diagrams of the general form

$$\Sigma = \sum K' G \tilde{V} G \tilde{V} \cdots \tilde{V} G K'^\dagger . \tag{B1}$$

It therefore follows that

$$\frac{1}{2i}(\Sigma - \Sigma^\dagger) = \frac{1}{2i} \sum (K' G \tilde{V} G \tilde{V} \cdots \tilde{V} G K'^\dagger - K' G^\dagger \tilde{V} G^\dagger \tilde{V} \cdots \tilde{V} G^\dagger K'^\dagger) . \tag{B2}$$

A typical term in this summation can be rewritten as a sum of terms containing $Y = (1/2i)(G - G^\dagger)$, as is illustrated by

$$\begin{aligned} &(1/2i)(K' G \tilde{V} G \tilde{V} G K'^\dagger - K' G^\dagger \tilde{V} G^\dagger \tilde{V} G^\dagger K'^\dagger) \\ &\quad = K' Y \tilde{V} G \tilde{V} G K'^\dagger + K' G^\dagger \tilde{V} Y \tilde{V} G K'^\dagger + K' G^\dagger \tilde{V} G \tilde{V} Y K'^\dagger . \end{aligned} \tag{B3}$$

Thus, for each diagram included in Σ, there appears in $\Sigma - \Sigma^\dagger$ a sum of terms formed by in-

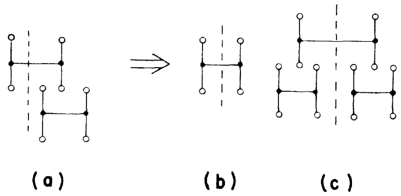

FIG. 7. Pair diagram (a), and the two new diagrams (b) and (c) which are generated by using the diagram parts to the left and right of the dotted line in (a) on both sides.

serting $Y = G - G^{\dagger}$ for a propagator G, and requiring that each propagator to the left (right) of this insertion has the value $G^{\dagger}(G)$. Now, since $Y < 0$, $\mathrm{Im}\Sigma$ will be negative definite if the sum (B2) can be factored such that

$$\mathrm{Im}\Sigma = U^{\dagger} Y U . \tag{B4}$$

From (B3) it is seen that this will be true if the irreducible diagrams included in the particular approximation are symmetric in the following sense: If a particular diagram included in the approximation is written in the form AGB, then the diagrams AGA, BGA, and BGB must also be included (here A and B refer to the parts of the diagram to the left and right of G, respectively, excluding K' and $K'^{\dagger}$). In Mills's terminology, no new diagrams are formed by "cutting" existing diagrams, and forming all possible diagrams from the pieces. For example, in Fig. 7, the inclusion of the pair diagram (a), by this rule, requires the inclusion of the single-site diagram (b) and the additional pair diagram (c). Diagram (c), in turn, requires the inclusion of more complex pair diagrams.

This symmetry rule was satisfied in the CPA, the traveling cluster approximation of Ref. 11, and in this work. The generalization of this argument to self-consistent skeleton graphs is straightforward and is also discussed in Ref. 11.

APPENDIX C

$P^{\sigma}G^{\sigma}P^{\sigma}$ can be evaluated in terms of G and $\tilde{\Sigma}^{\sigma}$ by straightforward matrix manipulation. Let

$$\tilde{\Sigma}^{\sigma} = \begin{pmatrix} \Sigma_1^{\sigma} & \Sigma_3^{\sigma} \\ \Sigma_3^{\sigma\dagger} & 0 \end{pmatrix}, \tag{C1a}$$

$$\overline{G} = \begin{pmatrix} G_1 & G_3 \\ G_3^{\dagger} & G_2 \end{pmatrix}, \tag{C1b}$$

and

$$G^{\sigma} = \begin{pmatrix} G_1^{\sigma} & G_3^{\sigma} \\ G_3^{\sigma\dagger} & G_2^{\sigma} \end{pmatrix}, \tag{C1c}$$

where G^{σ} is projected onto a 2×2 matrix in the same manner as $\tilde{\Sigma}^{\sigma}$ and $\overline{G}$ were projected in Sec. III. $G_1^{\sigma} = P^{\sigma}G^{\sigma}P^{\sigma}$, $G_2^{\sigma} = (1 - P^{\sigma})G^{\sigma}(1 - P^{\sigma})$, and $G_3^{\sigma} = P^{\sigma}G^{\sigma}(1 - P^{\sigma})$. Note we have included the fact that $\Sigma_2^{\sigma} = 0$ [Eq. (3.15b)]. From Eq. (3.13) we have

$$G^{\sigma} = \overline{G}(I + \tilde{\Sigma}^{\sigma}\overline{G})^{-1} . \tag{C2}$$

Substituting the matrix forms and performing the matrix manipulation, we obtain

$$G_1^{\sigma} = [G_1 - G_3(1 + \Sigma_3^{\sigma\dagger}G_3)^{-1}\Sigma_3^{\sigma\dagger}G_1][1 + \Sigma_1^{\sigma}G_1 + \Sigma_3^{\sigma}G_3^{\dagger} - (\Sigma_1^{\sigma}G_1 + \Sigma_3^{\sigma}G_2)(1 + \Sigma_3^{\sigma\dagger}G_3)^{-1}\Sigma_3^{\sigma\dagger}G_1]^{-1} = \overline{X}D^{-1} , \tag{C3}$$

where

$$\begin{aligned} \overline{X} &= [1 - G_3(1 + \Sigma_3^{\sigma\dagger}G_3]^{-1}\Sigma_3^{\sigma\dagger}]G_1 \\ &= [1 - (G_3 - G_3\Sigma_3^{\sigma\dagger}G_3 + \cdots)\Sigma_3^{\sigma\dagger}]G_1 \\ &= [1 - G_3\Sigma_3^{\sigma\dagger} + (G_3\Sigma_3^{\sigma\dagger})^2 - \cdots]G_1 \end{aligned}$$

or

$$\overline{X} = (1 + G_3\Sigma_3^{\sigma\dagger})^{-1}G_1 , \tag{C4}$$

and where

$$\begin{aligned} D &= \{1 + \Sigma_1^{\sigma}G_1 - \Sigma_1^{\sigma}G_1(1 + \Sigma_3^{\sigma\dagger}G_3)^{-1}\Sigma_3^{\sigma\dagger}G_1 + \Sigma_3^{\sigma}[G_3^{\dagger} - G_2(1 + \Sigma_3^{\sigma\dagger}G_3)^{-1}\Sigma_3^{\sigma\dagger}G_1]\}^{-1} \\ &= [1 + \Sigma_1^{\sigma}(1 + G_3\Sigma_3^{\sigma\dagger})^{-1}G_1 + \Sigma_3^{\sigma}G_3^{\dagger} - \Sigma_3^{\sigma}G_2\Sigma_3^{\sigma\dagger}(1 + G_3\Sigma_3^{\sigma\dagger})^{-1}G_1]^{-1} \end{aligned}$$

or

$$D = [1 + (\Sigma_1^{\sigma} - \Sigma_3^{\sigma}G_2\Sigma_3^{\sigma\dagger})\overline{X} + \Sigma_3^{\sigma}G_3^{\dagger}]^{-1} . \tag{C5}$$

APPENDIX D: PHONON DENSITY OF STATES

The density of states $v(\omega)$ for a phonon system can be determined from the displacement-displacement Green's function G by the relation

$$v(\omega) = -\frac{1}{\pi d s}\frac{1}{N}\lim_{z\to\omega^2+i0^+}\operatorname{Im}\sum_i [\overline{MG}(z)]_{ii}\,, \tag{D1}$$

where M is the mass matrix [see Eq. (2.3)], s is the number of atoms per unit cell, d is the dimensionality of the system, and N is the number of sites. In the augmented space we have

$$[\overline{MG}(z)]_{ii} = \langle if\,|\hat{M}\hat{G}(z)\,|\,if\rangle \tag{D2}$$

and

$$\langle if_\sigma|\hat{M}|jf_{\sigma'}\rangle = \begin{cases} \bar{u}\delta_{ij}, & \sigma=\sigma'=\phi \\ u'\delta_{ij}, & \sigma=\phi,\ \sigma'=i \\ \tilde{u}\delta_{ij}, & \sigma=\sigma'=i \end{cases} \tag{D3}$$

where $\bar{u}$, u', and $\tilde{u}$ are defined in Eq. (5.5). Substituting (D3) into (D2) we obtain

$$\begin{aligned}\frac{1}{N}\sum_i \langle if\,|\hat{M}\hat{G}\,|\,if\rangle &= \frac{1}{N}\sum_i \langle if\,|\hat{M}\,|\,if\rangle\langle if\,|\hat{G}\,|\,if\rangle \\ &\quad + \frac{1}{N}\sum_i \langle if\,|\hat{M}\,|\,if_i\rangle\langle if_i\,|\hat{G}\,|\,if\rangle\,, \\ &= \bar{u}\overline{G}_{00} + \frac{1}{N}u'\sum_i \langle if_i\,|\hat{G}\,|\,if\rangle\,.\end{aligned} \tag{D4}$$

In order to evaluate $(1/N)\sum_i \langle if_i|\hat{G}|f_i\rangle$, we use the 2×2 block notation defined in Eq. (2.2) for the operators $\hat{G}$ and $\hat{K}=\hat{G}^{-1}$. Then

$$G'^{\dagger} = -\tilde{K}^{-1}K'^{\dagger}\overline{G} = -FK'^{\dagger}\overline{G}\,, \tag{D5}$$

where we set $F=\tilde{K}^{-1}$ to correspond with the notation used in Secs. II and III. Using the above expression we find

$$\frac{1}{N}\sum_i \langle if_i\,|\hat{G}\,|\,if\rangle = \frac{1}{N}\sum_i\sum_{lu}\sum_{jn} F_{ij}^{\sigma_1(i),\sigma_u(l)}K'^{\dagger\,\sigma_u(l)}_{jn}\overline{G}_{ni}\,.$$

If we Fourier transform on the sites in the disorder space according to Eq. (3.8), we have

$$\frac{1}{N}\sum_i \langle if_i\,|\hat{G}\,|\,if\rangle = \frac{1}{N}\sum_i\sum_{jnl}\sum_u\sum_{\vec{q}} F(\vec{q})^{\sigma_1,\sigma_u}_{0,j-l}\,e^{i\vec{q}\cdot\vec{R}_{il}}K'^{\dagger\,\sigma_u}_{j-l,n-l}\overline{G}_{ni}\,.$$

If we now Fourier transform $\overline{G}$ on the real-site indices, the equation can be reduced to the form

$$\frac{1}{N}\sum_i \langle if_i\,|\hat{G}\,|\,if\rangle = \sum_u\sum_{ss'}\sum_{\vec{q}} F(\vec{q})^{\sigma_1,\sigma_u}_{0,s'}K'^{\dagger\,\sigma_u}_{s',s}\,e^{i\vec{q}\cdot\vec{R}_{s0}}\,\overline{G}(\vec{q})\,.$$

All the terms on the right-hand side are given or are computed in the process of evaluating $\overline{G}$. These results apply to any level approximation (single-site, pair, etc.) as long as we set $\sigma_1(i)=\{i\}$.

---

*Present address: Sektion Physik der Universität München, Theoretische Physik, Theresienstr. 37, D-8000 München 2, West Germany.

[1] For a complete review through 1973 see R. J. Elliott, J. A. Krumhansl, and P. L. Leath, Rev. Mod. Phys. 46, 465 (1974).

[2] P. Soven, Phys. Rev. 156, 809 (1967).

[3] D. W. Taylor, Phys. Rev. 156, 1017 (1967).

[4] J. A. Blackman, D. M. Esterling, and N. F. Berk, Phys. Rev. B 4, 2412 (1971).

[5] H. Shiba, Prog. Theor. Phys. 46, 77 (1971).

[6] T. Kaplan and M. Mostoller, Phys. Rev. B 9, 1783 (1974).

[7] S. Takeno, Prog. Theor. Phys. 40, 942 (1968); L. Schwartz, H. Krakauer, and H. Fukuyama, Phys. Rev. Lett. 30, 746 (1973).

[8] B. G. Nickel and W.H. Butler, Phys. Rev. Lett. 30, 363 (1973).

[9] F. Ducastelle, J. Phys. C 7, 1795 (1974); J. Mertsching, Phys. Status Solidi B 63, 241 (1974).

[10] A. Gonis and J. W. Garland, Phys. Rev. B 18, 3999 (1978); C. W. Myles and J. D. Dow, Phys. Rev. Lett. 42, 254 (1979).

[11] R. Mills and P. Ratanavararaksa, Phys. Rev. B 18, 5291 (1978).

[12] A. Mookerjee, J. Phys. C 6, L205 (1973); 6, 1340 (1973).

[13] T. Kaplan and L. J. Gray, Phys. Rev. B 14, 3462 (1976).

[14] T. Kaplan and L. J. Gray, Phys. Rev. B 15, 3260 (1977).

[15] H. W. Diehl and P. L. Leath, Phys. Rev. B 19, 587 (1979).

[16] H. W. Diehl and P. L. Leath, Phys. Rev. B 19, 596 (1979).

[17] H. W. Diehl, P. L. Leath, and T. Kaplan, Phys. Rev. B 19, 5044 (1979).

[18] R. J. Elliott and D. W. Taylor, Proc. R. Soc. London A296, 161 (1967).

[19] P. L. Leath and B. Goodman, Phys. Rev. 181, 1062 (1969).

[20] T. P. Schultz and D. Shapiro, Phys. Rev. B 7, 5090 (1973).

[21] A. Mookerjee, J. Phys. C 8, 1524 (1975); 8, 2943 (1975).

[22] P. Dean, Proc. R. Soc. London A260, 262 (1961); Rev. Mod. Phys. 44, 127 (1972).

[23] P. R. Halmos, *Hilbert Space Problem Book* (Van Nostrand, New York, 1967).